Daniel Cernadas, Cristina Trillo, Ángel F. Doval, Benito V. Dorrío, Carlos López, José L. Fernández and Mariano Pérez-Amor, "Rayleigh Wave Amplitude Field Determination by a Simple Speckle Point Interferometer," in "Interferometry in Speckle Light: Theory and Applications", P. Jacquot y J.-M. Fournier, Eds., 297-304, Springer-Verlag 2000

http://dx.doi.org/10.1007/978-3-642-57323-1_37

Rayleigh Wave Amplitude Field Determination by a Simple Speckle Point Interferometer

Daniel Cernadas, Cristina Trillo, Ángel F. Doval, Benito V. Dorrío, Carlos López, José L. Fernández and Mariano Pérez-Amor

Dpto. de Física Aplicada. Universidad de Vigo. E.T.S. de Ingenieros Industriales y de Minas. Lagoas-Marcosende. 36200 Vigo (Spain)

Abstract. A very simple speckle point interferometer of the Michelson type and the method employed to achieve nanometric resolution and repeatability is described.
Among the subjects of interest, the selection of the dimensions of the detector compared to the speckle size and fringe separation and the effects of averaging the signal obtained from successive acquisitions under identical conditions are evaluated.
An application of the interferometer to the measurement of the amplitude field of a Rayleigh wave train, propagating on the surface of an aluminum slab, with nanometric resolution is presented. The average repeatability obtained is of the order of 2 nm.

1 Introduction

A lot of work has been devoted in the last decades to the measurements of microvibrations by laser interferometry. As a result, nowadays there is available a variety of methods suitable to measure mechanical displacements in the nanometer range with temporal bandwidth of tens of MHz, allowing the application of high industrial potential technologies like laser ultrasonics and laser Doppler velocimetry ([1], [2], [3]).

However, one of the main drawbacks for the wide spread application of these techniques is the relatively high cost and lack of compactness and robustness of the interferometers ([4]). For example, the standard velocity sensing interferometers, such as time-delay as well as Fabry-Pérot types, need a high mechanical stability and a very stable lasing frequency to work properly. On the other hand, displacement sensing reference beam interferometers (i.e. Michelson type) are more compact, cheaper, present a flat frequency response and impose less requirements about the laser frequency stability. Although this last type of interferometers is, in principle, more sensitive to low frequency noise due, for example, to mechanical unstability of the inspected surface, seismic and environmental perturbations, filtering procedures may be devised to cancel its effect on the measurements. Indeed, their fundamental limits of sensitivity are similar than for the velocity sensing interferometers [1].

In this context, the present work explores the performance limits of a Michelson interferometer in its simplest configuration (without any phase or frequency modulator, without polarising optics and using direct, non-differential detection and only a basic digital oscilloscope for the signal treatment) with the aim to measure Rayleigh wave fields.

Since about 1950 it was realised that surface waves like Rayleigh ones, could be used for non-destructive testing ([5]). This kind of elastic wave propagates along the surface of bodies. It can be shown that the propagation is nondispersive and its velocity is slightly less than the S shear waves, a class of bulk waves.

The energy associated with the Rayleigh waves is contained within a depth approximately equal to a wavelength. Then the waves are diffracted in two dimensions and the amplitudes of the field fall as $r^{-1/2}$ typically. By the other hand, the bulk waves fall as r^{-1}, where r is the distance to the source. Also, since the propagation of Rayleigh waves occur along the surface, the information that carry is easily accessible by different methods. One of the most powerful ones is the measurement of the instantaneous displacement field by some imaging technique like TV holography [6], or holographic interferometry [7]. Another optical possibility consists in sequentially scan the surface by point interferometry, repeating the excitation-measurement cycle at each point. For the most usual materials (metals, ceramics, etc.) these methods work in the MHz ultrasonic range.

2 Signal Calculation

The electric fields of the interfering beams at the detection plane $\mathbf{x}(x, y)$ of a speckle Michelson interferometer with reference beam (fig.1) can be expressed as

$$\mathbf{E}_i(\mathbf{x},t) = \mathbf{E}_{i0}(\mathbf{x},t)\exp(j\phi_i) \quad i = 1,2 \tag{1}$$

where

$$\phi_1(\mathbf{x},t) = k_0 L_1(\mathbf{x},t) - \omega t + \phi_{10}(t) + \psi_p(\mathbf{x}) \tag{2}$$

$$\phi_2(\mathbf{x},t) = k_0 L_2(\mathbf{x},t) - \omega t + \phi_{20}(t) \tag{3}$$

where $\mathbf{E}_{10}(\mathbf{x},t)$ is the amplitude of the object beam, $\mathbf{E}_{20}(\mathbf{x},t)$ is the amplitude of the reference beam, $k_0 = 2\pi / \lambda_0$ is the wave number in vacuum, $\omega / 2\pi = \nu$ is the optical frequency, $L_i(\mathbf{x},t)$ is the optical path of the beam "i" from the source to the point $\mathbf{x}$, $\phi_{i0}(t)$ is a phase term that takes in account the phase at the source and $\psi_p(\mathbf{x})$ is a random phase term due to the surface roughness of the object OB.

The irradiance of each beam at a given point is

$$I_i(\mathbf{x},t) = <(\mathbf{E}_i(\mathbf{x},t) \bullet \mathbf{E}_i^*(\mathbf{x},t)> \quad i = 1,2 \tag{4}$$

where < > means temporal average. The total irradiance is,

$$I_s = I_1 + I_2 + 2 < \mathrm{Re}\left\{\mathbf{E}_{10} \bullet \mathbf{E}_{20}^* \exp[j(\phi_1 - \phi_2)]\right\}> \tag{5}$$

where the dependence $(\mathbf{x},t)$ is suppressed for alleviating notation.

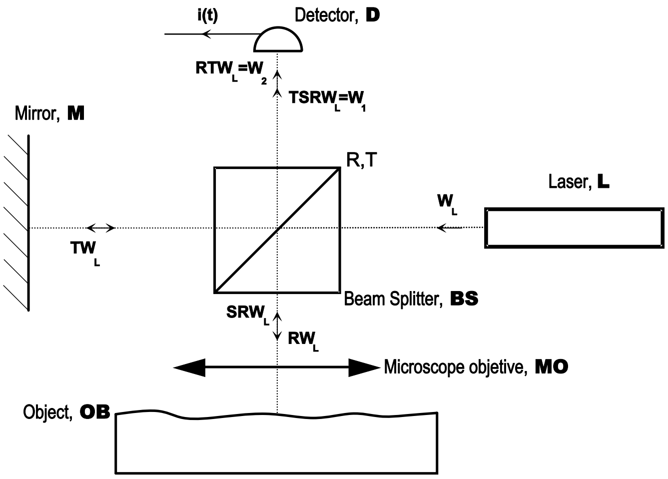

Fig.1. Layout of the Michelson speckle interferometer.

Assuming that both beams are linearly polarised with $\mathbf{E}_i$ parallel vectors, we can write

$$I_s = I_1 + I_2 + 2 < E_{10} E_{20}^* \cos(\phi_1 - \phi_2) > \tag{6}$$

and, if the averaging time is shorter than the temporal scale of the variation of $L_1 - L_2$, then

$$I_s(\mathbf{x},t) = I_1(\mathbf{x},t) + I_2(\mathbf{x},t) + 2\sqrt{I_1(\mathbf{x},t) I_2(\mathbf{x},t)}\,|\gamma| \cos[\phi_1(\mathbf{x},t) - \phi_2(\mathbf{x},t) + \mathrm{Arg}(\gamma)] \tag{7}$$

where γ is the complex degree of coherence, that remains practically constant if the variation of optical path imbalance $L_1 - L_2$ is much smaller than the laser coherence length [8]. Also, $\phi_{10} - \phi_{20}$ vanished in the averaging process.

The detector output current will contain a signal term, i_s, proportional to the optical power W_s reaching its sensitive area Σ_d :

$$i_s(t) = \mathbb{R} W_s(t) \tag{8}$$

where $\mathbb{R}$ is the responsivity, and

$$W_s(t) = \int_{\Sigma_d} I_s(\mathbf{x},t) da = W_1(t) + W_2(t) + W_{12}(t) \tag{9a}$$

$$W_i(t) = \int_{\Sigma_d} I_i(\mathbf{x},t) da \,, \tag{9b}$$

$$W_{12}(t) = 2|\gamma| \int_{\Sigma_d} \sqrt{I_1(\mathbf{x},t) I_2(\mathbf{x},t)} \cos[\phi_1(\mathbf{x},t) - \phi_2(\mathbf{x},t) + \mathrm{Arg}(\gamma)] da \quad (9c)$$

In practice, for the object OB displacements in the nanometer range, the object beam at the detector plane can be described as a smooth wavefront $\phi_{W_1}(\mathbf{x})$ with a superimposed random term $\psi_p(\mathbf{x})$, being both stationary. Also, the reference wavefront at the detector can be described by a stationary term $\phi_{W_2}(\mathbf{x})$. So,

$$k_0 L_1(\mathbf{x},t) = \phi_{W_1}(\mathbf{x}) + k_0 L_{10}(0,t) + \mathbf{G} \bullet \mathbf{u}(t) \quad (10)$$

$$k_0 L_2(\mathbf{x},t) = \phi_{W_2}(\mathbf{x}) + k_0 L_2(0,t) \quad (11)$$

where $L_{10}(0,t)$ is the path length at the detector centre for the position at rest of surface OB, $\mathbf{u}$ is the instantaneous displacement vector of this surface at the measuring point, and $\mathbf{G}$ is the sensitivity vector (fig.2.a), given by the difference between illumination and observation wave vectors at the OB surface

$$\mathbf{G} = \mathbf{k}_{ill} - \mathbf{k}_{obs} \quad (12)$$

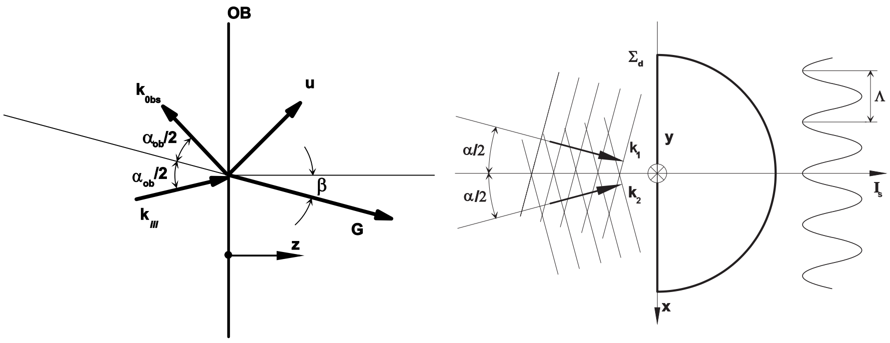

Fig.2. (a) Illumination-observation geometry. (b) Geometry of the wavefronts reaching the detector for the case of a tilt α.

In the out-of-plane configuration, $\beta = 0$ and the mean phase variation of the reflected wave front is

$$\mathbf{G} \bullet \mathbf{u}(t) = (4\pi/\lambda) z(t) \quad (13)$$

So, denominating $L(0,t) = L_{10}(0,t) - L_2(0,t)$ and $\phi_W = \phi_{W_1} - \phi_{W_2}$, the evaluation of $W_{12}(t)$ can be done as follows:

$$W_{12}(t) = 2|\gamma| \int_{\Sigma_d} \sqrt{I_1(\mathbf{x},t) I_2(\mathbf{x},t)} \times \cos[k_0 L(0,t) + \phi_W(\mathbf{x}) + (4\pi/\lambda) z(t) + \psi_p(\mathbf{x}) + \mathrm{Arg}(\gamma)] da$$

$$\Rightarrow W_{12}(t) = 2|\gamma| \sum_{n=1}^{N} \sqrt{I_{1n}(t) I_{2n}(t)} M_n(t) \tag{14}$$

where $M_n(t) = \int_{\Sigma_n} \cos[\phi_W(\mathbf{x}) + \phi_{pn}(t)] da$ (15)

fulfilling $-1 \le (M_n(t)/\Sigma_n) \le 1$ (16)

and $\phi_{pn}(t) = k_0 L(0,t) + (4\pi/\lambda) z(t) + \psi_{pn} + \mathrm{Arg}(\gamma)$ (17)

In the expression (14), N is the number of speckles in Σ_d. Also ϕ_{pn}, I_{1n} and I_{2n} are all assumed to be constant in each speckle area Σ_n. The value of M_n depends strongly on the form of the function $\phi_W(\mathbf{x})$. For example, if the local mismatch between wavefronts at the speckle "*n*" is a tilt (fig.2.b), then $\phi_{Wn}(\mathbf{x}) = (\mathbf{k}_{1n} - \mathbf{k}_{2n}) \bullet \mathbf{x}$ and a straight fringe pattern of period

$$\Lambda = \frac{2\pi}{\nabla \phi_{Wn}} = 2\pi / |\mathbf{k}_{1n} - \mathbf{k}_{2n}| = \frac{\lambda}{2\sin(\alpha/2)} \tag{18}$$

is observed into each speckle (fig.3.a). Approximating the speckle area Σ_n by a circle of diameter s_n, with centre at $\mathbf{x}_{on}$, (15) turns out

$$M_n(t) = \frac{\pi s_n^2}{4} \cos[(\mathbf{k}_{1n} - \mathbf{k}_{2n}) \bullet \mathbf{x}_{on} + \phi_{pn}(t)] \frac{2\,\mathrm{J}_1(\pi s_n/\Lambda_n)}{(\pi s_n/\Lambda_n)} \tag{19}$$

where $\mathrm{J}_1(\,)$ is a Bessel function of the first kind and order 1. So, for $s_n > \Lambda_n$, the interference term practically vanishes, which gives a criterion for the maximum allowable misalignment, α_{max}, between the object and reference beams, in function of the speckle average diameter s:

$$\sin(\alpha_{max}/2) < (\lambda/2s) \tag{20}$$

In a more general case, we can write

$$M_n(t) = \frac{\pi s_n^2}{4} f_n(\phi_{wn}, s_n) \cos[\phi_{pn}(t) + \phi_{fn}(\phi_{wn}, \mathbf{x}_{on})] \tag{21}$$

where $|f_n| \le 1$ and the function ϕ_{wn} may take in account a curvature mismatch between both wavefronts (fig.3c). So, from (14) and (21)

$$W_{12}(t) = 2|\gamma| \sum_{n=1}^{N} A_n(t) \cos[\phi_{dn}(t) + \psi_{pn}] = 2|\gamma| A \cos\phi \tag{22}$$

with

$$A_n(t) = \sqrt{I_{1n}(t) I_{2n}(t)} f_n \frac{\pi s_n^2}{4} \quad \text{and} \quad \phi_{dn}(t) = \phi_{pn}(t) + \phi_{fn} - \psi_{pn} \tag{23}$$

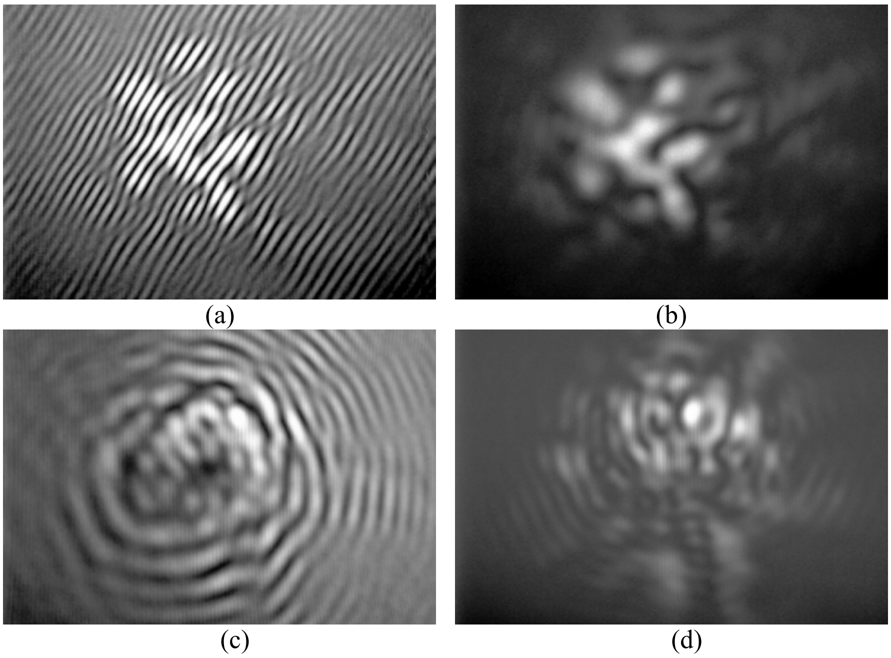

Fig.3. Fringe patterns (left) corresponding to the superposition of a speckle pattern (right) with a plane reference wavefront. (a) Nearly plane speckle wavefront. (c) Spherical speckle wavefront obtained by defocusing the objective MO.

The phasor $A\exp(j\phi)$ is the superposition of the phasors $A_n \exp[j(\phi_{dn} + \psi_{pn})]$, and both can be described as random variables. Assuming that I_{2n}, s_n and f_n are constant over the detector whole aperture, and taking in account $\sqrt{I_{1n}} = E_{10n}$

$$A_n(t) = \sqrt{I_2(t)}\,\frac{\pi s^2}{4}\,f(\phi_w, s)E_{10n}(t) \tag{24}$$

and E_{10n} (the speckle amplitude) has a Rayleigh distribution with mean value

$$\bar{E}_{10n} = \sqrt{\frac{\pi \bar{I}_1}{4}} \tag{25}$$

being $\bar{I}_1 = W_1 / \Sigma_d$. Also, A has a Rayleigh distribution whose mean value and variance are:

$$\bar{A} = \frac{\pi s^2}{4} f \sqrt{\bar{I}_1 I_2 \frac{\pi N}{4}} \tag{26}$$

$$\sigma^2(A) = \left[\frac{\pi s^2}{4} f\right]^2 \bar{I}_1 I_2 \left(1 - \frac{\pi}{4}\right) N \tag{27}$$

From (8), (9) and (26) the mean detector output is

$$i_s(t) = \mathbb{R} W_{so}(t)\left[1 + m(t)\cos\left(k_o L(0,t) + \frac{4\pi}{\lambda} z(t) + \psi'_p\right)\right] \tag{28}$$

with $W_{so}(t) = W_1(t) + W_2(t)$ (29)

$$m(t) = \frac{2|\gamma| f(\phi_w, s)\sqrt{\frac{\pi}{4N}}\sqrt{W_1(t)W_2(t)}}{W_1(t) + W_2(t)} \tag{30}$$

and ψ'_p is a random value with uniform probability density in $[-\pi, \pi]$.

3 Signal-to-noise ratio

The power signal to noise ratio for a full excurssion of the phase is, assuming photon shot noise limited detection

$$\left.\frac{S}{N}\right|_{power} = \frac{\mathbb{R} W_{so}^2 \frac{m^2}{2}}{2e\Delta f W_{so}} = \frac{\eta W_{so} m^2}{4h\nu\Delta f} = \frac{\eta}{h\nu\Delta f}\frac{S}{S+1} RTW_L |\gamma|^2 \left[f\sqrt{\frac{\pi}{4N}}\right]^2 \tag{31}$$

where η is the quantum efficiency, e the electron charge, Δf the bandwidth, h the Planck constant, W_L the laser power, T the transmittance and R the reflectance of the beam splitter BS, and S the power reflection ratio for the object beam. The number N of speckles may be estimated by:

$N \cong \frac{1 - \cos\theta_{MO}}{1 - \cos(\lambda / \pi ro)} \cong \frac{2\pi^2 r_o^2}{\lambda^2}[1 - \cos\theta_{MO}]$, with r_o the illuminated spot radius at object surface, $n \sin\theta_{MO} = \text{NA}$ the numerical aperture of the objective MO and n the refraction index at the object location.

For a small signal amplitude $z(t) << \lambda / 4\pi$, and the interferometer working at the quadrature point, the cosine term in (28) may be substituted by $4\pi z / \lambda$, for which the minimum detectable displacement (for $S/N = 1$), z_{min}, is:

$$z_{min} = \frac{\lambda}{4\pi}\sqrt{\frac{h\nu\Delta f(1+S)}{\eta SRTW_L}}\frac{1}{|\gamma|}\frac{1}{f}\sqrt{\frac{4N}{\pi}}$$

For the parameters of the interferometer, $W_L = 5mW$, $\lambda = 633nm$, $\text{NA} = 0.32$, it turns out that, for $r_o = 0.05mm$, $N = 6400$ and $z_{min} = 0.3nm$.

4 Averaging noise

The effect of averaging on the noise can be evaluated taking in account that uncorrelated variations in the average of K samples decay as $\sqrt{K}$ (fig.4).

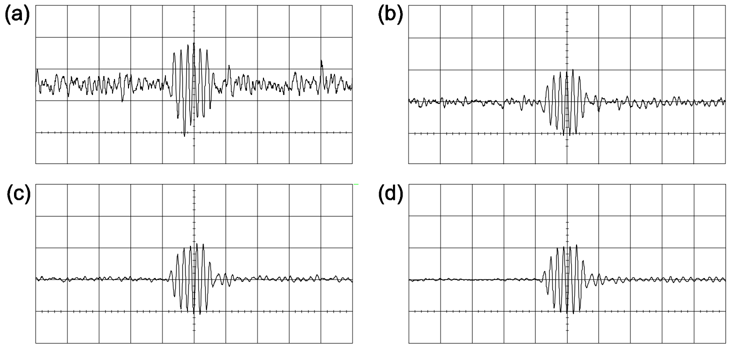

Fig.4. Traces of the interferometer output for a 20nm peak-to-peak Rayleigh wave of 1MHz frequency. (a) no averaging K=1, (b) K=4, (c) K=16 and (d) K=64.

Acknowledgements

We acknowledge the support of the CICYT (proj. TAP-1999-1167-C03-01). Supplementary founding from the *Universidad de Vigo* (proj. 64102I022) is also acknowledged.

References

1. C. Scruby, L. Drain: *Lasers Ultrasonics, Techniques and Applications* (Adam Hilger, Bristol 1990)
2. R. Dewhurst and Q. Shan: Optical remote measurement of ultrasound. Meas. Sci. Technol. **10**, R139-R168 (1999)
3. D. Williams: *Optical Methods in Engineering Metrology* (Chapman & Hall, London 1993)
4. M. Hatcher: Laser ultrasonic: a revolutiong in waiting. Opto & Laser Europe , 18-21 May (2000)
5. D. Royer, E. Dieulesaint: *Elastic Waves in Solids I & II* (Springer-Verlag, Berlin-Heidelberg 2000)
6. A. Doval: A systematic approach to TV holography. Meas. Sci. Technol. **11,** R1-R36 (2000)
7. F. Schroeder and H. Crostack: Real-time holography of ultrasonic surface waves. Proc. SPIE Vol. 2782, 290-295 (1996)
8. M. Born and E. Wolf: *Principles of Optics* (Pergamon Press, Oxford 1970)
9. J.W. Goodman: *Statistical Optics*, 44-59 (J. Wiley and Sons, New York 1985)